Journal of Applied Polymer Science

Facile Covalent Surface Functionalization of Multiwalled Carbon Nanotubes with Poly(2-Hydroxyethyl Methacrylate) and Interface Related Studies When Incorporated into Epoxy Composites

Greg Curtzwiler,[1,3] Andreas Plagge,[1] Keith Vorst,[2,3] John Story[3,4]

[1]School of Polymers and High Performance Materials, University of Southern Mississippi, Hattiesburg, Mississippi 39406
[2]Department of Industrial Technology, California Polytechnic State University, Plastics and Packaging, San Luis Obispo, California 93407
[3]V Laboratories and Echo-Pac, California Polytechnic Technology Park, Building 83, San Luis Obispo, California 93407
[4]University of St. Thomas, Cameron School of Business, 3800 Montrose, Houston, Texas 77006
Correspondence to: K. Vorst (E-mail: kvorst@calpoly.edu)

ABSTRACT: Carbon nanotubes (CNTs) have seen increased interest from manufacturers as a nanofiber filler for the enhancement of various physical and mechanical properties. A major drawback for widespread commercial use has been the cost associated with growing, functionalizing, and incorporating CNTs into commercially available polymeric matrices. Accordingly, the main objective of this study was to investigate the effects of adding commercially viable functionalized multiwalled carbon nanotubes (MWCNT) to a commercially available epoxy matrix. The mechanical behavior of the nanocomposites was investigated by mechanical testing in tensile mode and fractures were examined by scanning electron microscopy. The thermal behavior was investigated by differential scanning calorimetry and thermogravimetric analysis. Molecular composition was analyzed by attenuated total reflectance Fourier transform infrared spectroscopy. Mechanical testing of the epoxy/functionalized-MWCNT indicated that the 0.15 wt % functionalized MWCNT composite possessed the highest engineering stress and toughness out of the systems evaluated without affecting the Young's modulus of the material. © 2012 Wiley Periodicals, Inc. J. Appl. Polym. Sci. 000: 000–000, 2012

KEYWORDS: nanotubes; graphene and fullerenes; composites; reinforcement; functionalization of polymers; coatings

Received 12 January 2012; accepted 9 August 2012; published online
DOI: 10.1002/app.38463

INTRODUCTION

The addition of carbon nanotubes (CNTs) to polymer matrices to increase the thermal, mechanical, and electrical properties of the resulting composite has been well documented.[1–16] For CNTs to effectively enhance the properties of a composite, the CNTs must be deagglomerated, well dispersed, and have sufficient interfacial interaction with the host matrix.[3,4,8–10,13,15,17–23] Both theoretical and experimental studies indicate that optimizing the polymer-CNT interface is essential to maximize substrate properties.[3,4,18,24] The most useful approach to increase interfacial interaction is chemical modification of the CNT to create functionality that has the potential to crosslink into the host matrix.[3,4,25,26] A CNT functionalization of only 1% of the surface's carbon atoms covalently linked into the host matrix can increase interfacial shear strength by over an order of magnitude without significantly decreasing CNT stiffness due to disruption of conjugation.[4,27] Several approaches have been employed to overcome the obstacles associated with CNT dispersion and deagglomeration with promising results.[3,4,8,19,28–30]

However, many of the processes developed to incorporate CNTs into high performance composites have difficulties when producing in commercial amounts due to the problems associated with incorporating CNTs into polymers. Carbon nanotubes have high aspect ratios and surface areas (over 1000 m^2 per g) and the high polarizability of the extended π-electron cloud yields large van der Waals forces (estimated to be 500 eV/micron of tube length) causing agglomeration thereby making complete exfoliation of bundled nanotubes a difficult challenge.[3,4,6,10,13,15,19,22,31] This tendency leads to a decrease of most of the critical properties of well-distributed CNTs. To form stable suspensions of CNTs in polymeric systems, the CNTs must be isolated, followed by a surface modification to inhibit reagglomeration and increase interactions with the host media for the application of interest.[3,4,19,28,32,33] The deagglomeration process is labor intensive and time consuming, hence

the ongoing inability to practically apply the potential of CNTs to commercial reality, even on a relatively small scale.

Many studies have indicated that chemical functionalization of the carbon nanotube sidewalls can significantly increase the interactions with the host matrix resulting in increased levels of dispersion.[1,4,7,8,13,15,19,21,24,27–30,32–36] For example, the addition of amino groups to double walled-carbon nanotubes (DWCNTs) increased dispersion over nonfunctionalized DWCNTs and increased fracture toughness over neat epoxy resin at loadings of ~1%.[4] Several labs have developed methods to achieve useful CNT material. However, the time consuming process of functionalization and preparation in a way that make production systems practical or economically viable, except in the most specialized applications, has yet to be realized. For example, Nguyen et al. and Wu et al. fabricated isocyanate functionalized MWCNTs and polystyrene functionalized MWCNTs that required 48 and 4 h, respectively, considering experimental setup, processing, and purification steps.[29,30] This setup and process time is still considered too costly for full production scale by many manufacturers.

The high aspect ratio, high strength, low density, and high stiffness are especially attractive attributes when considering use of CNT for polymer additives.[3,4,8,13,15,16,18,19,21] The potential mechanisms for mechanical enhancement include CNT pull-out (matrix debonding), CNT bridging, and crack deflection.[3,24,25,28] CNT bridging, in particular, causes the most enhancement in mechanical properties as a result of the high mechanical properties of the CNT. As the crack propagates through the polymer matrix, it approaches a CNT and transfers the load which dissipates energy and inhibits propagation.[24,28] For the CNT-bridging mechanism to dominate during a fracture event, the length of the CNT must be above a critical length as well as have sufficient interaction with the matrix and a high degree of dispersion.[24] Below these critical parameters, the dominating mechanism will probably be CNT pull-out. Above different critical conditions, the dominating mechanism will be a combination of CNT pull-out and rupture.[24]

The surface morphology of fractured, brittle materials, such as crosslinked epoxy networks, can be related to the macroscopically measured fracture properties as the released elastic energy can be equated to the surface energy for creating new crack surfaces.[16,37,38] In general, tougher materials possess rougher fractured surfaces; this correlates to requiring more work to propagate the crack.[16,26,37–39] The correlation between a fractured surface morphology and measured macroscopic properties of more ductile materials may be more complex due to plastic deformation as the work related to plastic deformation is much higher than the surface energy of the newly formed surface.[37] When a material is less prone to fracture, it will exhibit more variation within the microstructure compared to a surface that contains more smooth planes.[16,17,38] Perez et al reported significantly rougher surfaces for tougher CNT based composites when compared to the neat epoxy.[18] Rougher surfaces have also been attributed to a good adhesion between the host matrix and the nanoparticle.[17,26,33]

Previous research has suggested that coating MWCNTs with polymeric hydroxyethyl methacrylate increased the interactions between MWCNTs and a polyurethane matrix, which was realized via a commercially viable process.[32] Accordingly, the main objective of this study was to investigate the effects of adding commercially viable functionalized MWCNTs to a commercially available epoxy matrix for employment according to the manufacturer's cure schedule. The authors believe the functionalization process described in the current research to be more commercially viable than those described in the literature due to reduced functionalization time, reduced cost of starting materials, facile methodology, and ease of scale up manufacturing. The functionalization methodology has also allowed for the realization of enhanced mechanical and thermal properties and reduced carbon nanotube concentrations than those observed in the literature. The mechanical properties were determined by electromechanical testing in tensile mode and crack propagation was studied postfracture by scanning electron microscopy (SEM). The thermal transitions and thermal decomposition behavior were determined by differential scanning calorimetry (DSC) and thermogravimetric analysis (TGA), respectively. The molecular composition of the surface was investigated by attenuated total reflectance Fourier-transform infrared spectroscopy (ATR-FTIR).

METHODS AND MATERIALS

Materials

Purified, unbundled, multiwalled carbon nanotubes (MWCNT) were used as received from Ahwahnee Technology (San Jose, CA). The epoxy resin was EPON 8111 (Resolution Performance Products, Pueblo, CO) and had an epoxy equivalent weight (EEW) of 300–320 g/eq and a viscosity of 800–1100 cP at 25°C. The curing agent was Ancamine triethylene tetramine (TETA) (Air Products, Allentown, PA) and had active hydrogen equivalent weight of 27 g/eq and a viscosity of 20 cP at 25°C. All other items were used as received from commercially available sources and used without further purification.

Fabrication of Poly(hydroxyethyl methacrylate)-Coated Multiwalled Carbon Nanotubes

A 25-mL round bottom flask was loaded with MWCNT (380 mg), 2-hydroxyethyl methacrylate (HEMA) (10.0 g), tetrahydrofuran (THF) (10.0 g), ethyl acetate (10.0 g), and a magnetic stir bar. A 0.25 inch diameter, tapered tip sonication horn was submerged in the liquid. The mixture was sonicated with a Misonix Microson XL 2000 (Farmingdale, NY) equipped with a 0.25-inch tapered tip at 20 W for 5 min. Benzoyl peroxide (BPO) (100 mg) was dissolved in THF (1.0 g) and added to the reaction flask after the solution was allowed to cool to room temperature. The system was purged with nitrogen for 15 min, and then placed in an oil bath at 80°C for 10 min. No control experiments were performed as previous research has indicated that under the conditions employed in this study, the polymer is covalently attached to the MWCNT surface as according to the proposed mechanism in Figure 1.[32]

The highly viscous liquid was washed with a 50 vol % of THF/ethyl acetate solution three times. A wash cycle consisted of sonicating at 20 watts for 30 s in the washing solvent followed by 10 min of centrifugation at 4000 rpm. The supernatant was decanted off into a glass bottle and the pellet was resuspended in

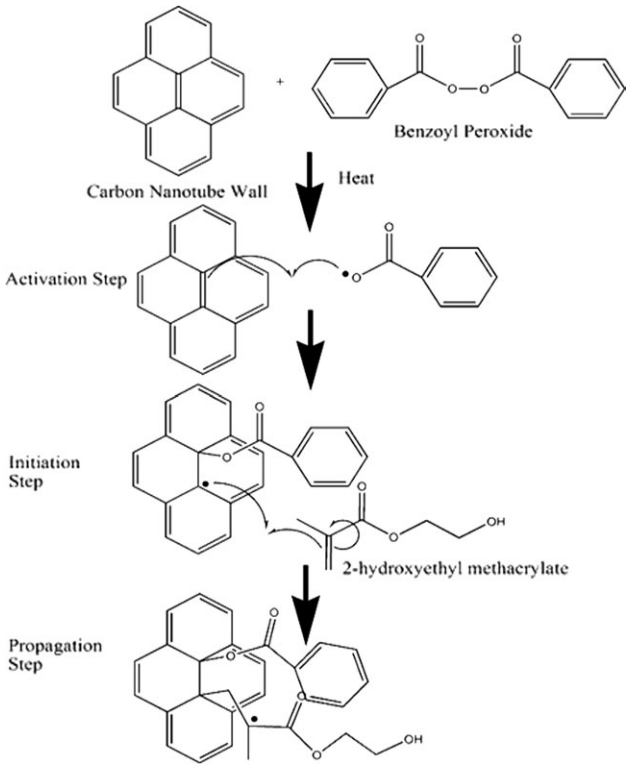

Figure 1. Proposal of mechanism for surface initiated polymerization of hydroxyethyl methacrylate from multiwalled carbon nanotube.

fresh solvent via tip sonication at 20 watts for 30 s. The poly (HEMA)-coated MWCNTs were determined to have a functionality of 30 wt % by TGA.

Fabrication of Poly(hydroxyethyl methacrylate)-Coated Multiwalled Carbon Nanotube/Epoxy Plaques

The functionalized MWCNTs from the pellet were sonicated in Ancamine TETA for 3 min at 20 watts such that plaques could be made containing 0.15 wt % and 1.0 wt % poly(HEMA) MWCNTS when cured. The poly(HEMA)-MWCNT functionalized TETA was mixed with EPON 8111 epoxy resin at the manufacturer's recommended stoichiometry for 1 min in a Thinky planetary mixer (model AR-100, Tokyo, Japan) followed by 30 s of defoaming then poured into a 8 in by 8 in polished aluminum mold and allowed to gel at room temperature. After the system gelled, it was placed into an oven at 100°C for 2 h.

Mechanical Analysis

The plaques were cut into rectangular strips that were ~200 mm long and 12.7 mm ± 0.1 mm wide via waterjet (Motive Systems, Paso Robles, CA). The strips were allowed to condition at 23°C and 50% relative humidity for 24 h prior to testing. The mechanical analysis was performed at 23°C and 50% relative humidity with a Testometric Universal Testing Machine (Model M350-5kN, Lancashire, UK) equipped with a 500 kgf load cell in tensile mode. The machine had a capacity of 5 kN with an accuracy of ± 0.5%. The rate of grip separation was 50.0 mm/min with a gauge length of 76.2 mm (3.0 in). The stress and strain at the proportional limit (PL), yield stress and strain, elastic modulus, and toughness were calculated from the force-deformation curves obtained from five specimens per epoxy plaque type. The toughness was estimated utilizing the trapezoidal rule.

Hardness

The hardness of each plaque was examined using a Vogel Measurements Shore D durometer at 20°C and 60% relative humidity according to ASTM D 2240. Each system was tested 10 times in random locations to ensure proper representation of the hardness properties.

Thermal Gravimetric Analysis

The thermal stability of each epoxy type was determined through TGA and is defined as the temperature at which the relative weight loss is two percent. The derivative of the relative weight loss curve with respect to temperature at a heat rate of 20°C per minute was utilized to observe the onset of major thermal decomposition steps. The peak of the derivative with respect to temperature was utilized to determine the temperature at which the maximum rate of thermal decomposition was observed.

Samples were obtained of each poly(HEMA)-MWCNT/epoxy composite and analyzed for the temperatures associated with the 2% weight loss, 5% weight loss, and the maximum peak derivative of the signal utilizing a Q500 TGA analyzer (TA Instruments, DE) and TA Universal Analysis software 4.5A for evaluation. The flow rate of the nitrogen (industrial grade, Air Gas, San Luis Obispo, CA) purge gas was 20 mL/min and the furnace was set to increase the temperature at a rate of 20°C/min.

Differential Scanning Calorimetry

DSC experiments were performed to determine first and second order thermal transitions of the poly(HEMA)-MWCNT/epoxy composites between −70°C and 150°C. Samples obtained from the prepared epoxy/poly-HEMA-MWCNT containing 0, 0.15, and 1.0 wt % MWCNT were placed in separate aluminum pans and nonhermetically sealed. Thermal transitions were evaluated on a TA Instruments Calorimeter model DSC Q2000 (TA Instruments, DE). The poly(HEMA)-MWCNT experiments consisted of a heat/cool/heat cycle between −70 and 150°C at a rate of 20°C/min in accordance with ASTM D3418-03.[40] The nitrogen flow rate inside the calorimeter cell was set to 50 mL/min and was supplied by a nitrogen generator (Domnick Hunter, model G5010W, Birtley, UK) with a purity of 99.999% N_2.

Attenuated Total Reflectance-Fourier Transform Infrared Spectroscopy

The molecular composition of the surfaces was examined using ATR-FTIR spectroscopy. Each scan consisted of measurements between 4000 and 650 cm^{-1} into a ZnSe based ATR crystal with dimensions 80 x 10 x 4 mm^3 and 45° face angle. Each spectrum consisted of 100 scans and was rationed versus a background spectrum. The latter was obtained prior to analyzing the samples and consisted of 100 scans. The spectra were obtained from the cast plaque comprised of poly(HEMA)-MWCNT/epoxy composites utilized for mechanical testing. A Pike Horizontal Attenuated Total Reflectance assembly, model 8224, was attached to a Digilab FT-IR FTS 2000 spectrometer. To avoid atmospheric contaminants a constant purge flow with

dried nitrogen and flow rate of 30 ml/min was applied during the analyses. All obtained final spectra were corrected for baseline and for optical distortions using Digilab software Win IR-pro 3.6.

Scanning Electron Microscopy

The surface characteristics of the fractured surface of the plaques were investigated utilizing an FEI Quanta 200 scanning electron microscope at an electron acceleration voltage of 20 kV. The surface of the fractured plaques was sputter-coated with a ca. 10nm thick gold coating using an Emitech K550X sputter coater and Ar as process gas. All images were obtained with the electron beam normal to the fractured surface.

RESULTS

Attenuated Total Reflectance-Fourier Transform Infrared Spectroscopy

ATR-FTIR spectroscopy experiments were conducted to determine the molecular composition of the surface of the carbon nanotube raw material, functionalized MWCNTs, and epoxy composites.

Figure 2 illustrates ATR-FTIR spectra I for raw MWCNT, and II for poly(HEMA)-modified MWCNT and transmission IR spectrum III of neat poly(HEMA) as a reference material. As can be seen when comparing the IR fingerprint region between 1300 and 1000 cm^{-1} in Figure 2, ATR-FTIR spectrum II and IR transmission spectrum III are complimentary and the relative intensity was determined by integration of bands. In this fingerprint region, band intensities A through D follows sequence B > C > A > D for both IR spectra II and III. In contrast, IR

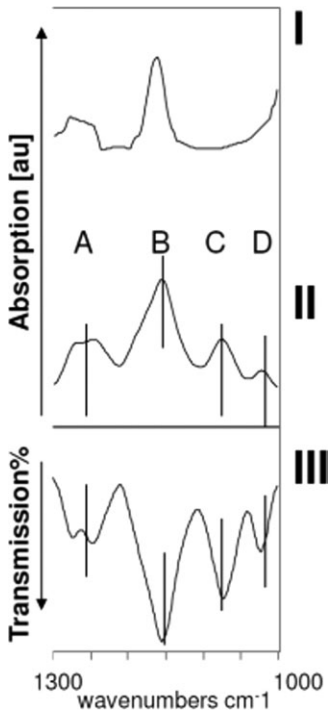

Figure 2. Comparison of IR fingerprint region between 1300 and 1000 cm^{-1} ATR-FTIR spectra of raw MWCNT (I) and poly(HEMA)-modified MWCNT (II). Transmission FTIR spectrum of neat poly(HEMA) (III).

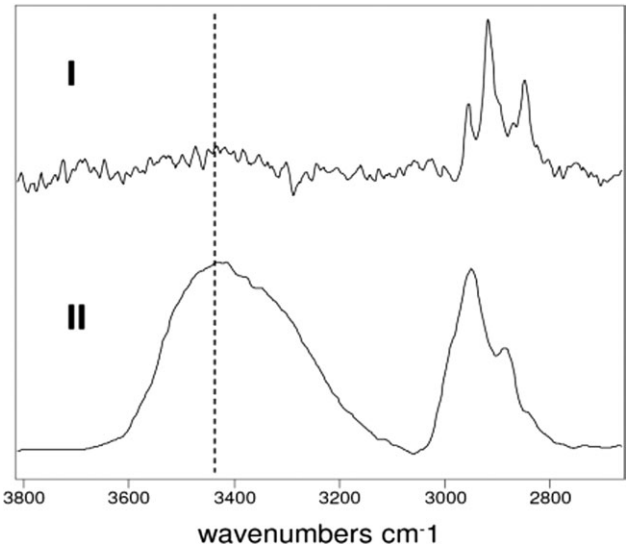

Figure 3. ATR spectra of raw MWCNT (I) and poly(HEMA)-modified MWCNT (II).

spectrum I (raw MWCNT), as illustrated in Figure 1(a) does not reveal this characteristic 4-band pattern. This indicates that the surface chemistry of modified MWCNT is defined by presence of OH-containing poly(HEMA) polymer which is expected to govern interface related chemistry.

It can also be seen in Figure 2 that IR spectrum I of raw MWCNT indicates a relative complex surface chemistry (with possibly oxygen related functional groups present). Because of the latter evaluation of an additional IR spectral range was necessary to specifically reveal OH content at raw versus modified MWCNT type.

This approach is seen in ATR-FTIR spectra of Figure 3. Hydroxyl content is illustrated by the band at ~3415 cm^{-1} (OH stretch) where trace I describes raw MWCNTs and IR trace II modified MWCNTs. Integration of the OH band area at about 3415 cm^{-1} was done for both IR traces I and II and each value was rationed versus integrated band area for alkyl related band (between approximately 3050–2770 cm^{-1}) present in each trace I and II of Figure 3. Such a procedure enables semiquantitative conclusions on OH content change for raw MWCNTs where a complex surface chemistry is indicated in IR spectra. The calculated ratio for modified MWCNTs was 2.2 versus 0.1 for raw MWCNT proving that the OH content in modified MWCNTs has significantly increased after poly(HEMA) was attached. Hydroxyl enriched surfaces on the modified MWCNTs should govern its interface chemistry.

The chemical effects of incorporating poly(HEMA)-modified MWCNT in different amounts in epoxy as additive is illustrated by compositional ATR-FTIR analysis in Figure 4, focusing on spectral range between 1800–750 cm^{-1}. For this IR study, protocols described by O'Brien/Hartman,[41] Dannenberg/Harp,[42] and Fountain[43] were used for band assignments and definition of functional groups typically present in crosslinked epoxy networks. As seen in IR trace I of Figure 4 composition and band pattern of composite with low concentration (0.15 wt %)

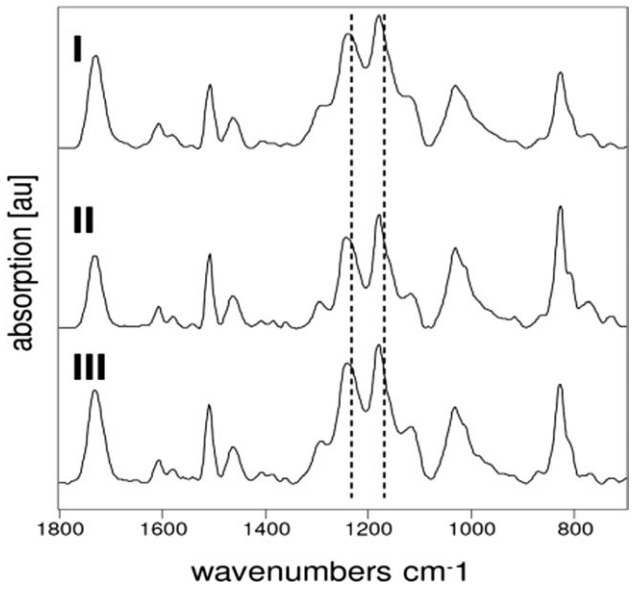

Figure 4. ATR-FTIR spectra of poly(HEMA)/MWCNT containing epoxy composites with 0.15 wt % (I) and 1 wt % (II). Trace III illustrates neat epoxy film.

poly(HEMA)/MWCNT is in close resemblance to neat epoxy, seen in trace III of Figure 4. However, the band pattern of the latter appears to be slightly different when compared with IR spectral pattern obtained from the higher 1 wt % poly(HEMA)/MWCNT concentration, seen in IR trace II of Figure 4.

In an approach to more precisely analyze how the modified MWCNT interface affects conversion in epoxy-composites when the polymer network is formed, a closer look at important IR spectral regions was investigated [Figure 5(a, b)]. In Figure 5(a), traces IA through IIIA of ATR-FTIR spectra illustrate overall concentration of OH groups in two epoxy composites and neat epoxy while IR traces IB through IIIB illustrate remaining oxirane concentration in crosslinked setups and are used to compare overall cure in epoxy, following.[42]

ATR-FTIR spectra in Figure 4(a) were used to semiquantify OH group concentration in epoxy composite networks. Standard procedure was to integrate the band of OH stretch at ~3360 cm^{-1} [highlighted in Figure 4(a)] and ratio versus integrated alkyl group band (between 3005 and 2800 cm^{-1}). These data are summarized in Table I. The calculation leads to a sequence where OH group concentration of neat epoxy >> 1 wt % > 0.15 wt %. Evaluation indicates the highest OH group concentration for neat epoxy, seen at trace IIIA of Figure 4(a) and lowest OH group concentration for composite with 0.15 wt %, seen in IR trace IA of Figure 4(a). Observation is supported by literature and that epoxy curing reaction between oxirane functional group and amine based hardener—seen in Figure 5 Scheme (a)—results in higher number of OH functional groups compared to curing reaction where oxirane groups react with OH groups as reactive specimen.[41] In latter curing scenario overall OH group concentration remains unchanged, illustrated by reaction the scheme in Figure 5(b).

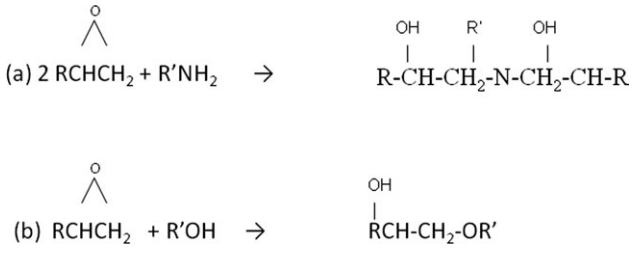

Figure 5. Potential reactions between oxirane groups and amines (a) and hydroxyls (b).[41]

Both curing reactions are simplified: for this reason, used multifunctional amine curing agent is illustrated with one amine group only in Figure 5 Scheme (a). Polyfunctional poly(-HEMA)-modified MWCNT is illustrated with single OH group in Figure 5 Scheme (b). The observation that final OH group concentration in cross-linked poly(HEMA)/MWCNT networks is smaller than for neat epoxy supports that modified and OH rich MWCNT interface successfully takes part in epoxy crosslinking reaction and becomes chemically attached to the epoxy network. Again, this can be concluded from ATR-FTIR spectra of Figure 6(a) and traces IA and IIA where relative intensity of OH bands is lower when compared with neat epoxy setup at IR trace IIIA.

An additional effort to determine how interface chemistry and presence of modified MWCNT affects curing rate in epoxy final content of oxirane group after crosslinking was analyzed and is illustrated by ATR-FTIR spectra of Figure 4(b) and traces 1B through IIIB. To semiquantify data, the band area for oxirane ring deformation at 915 cm^{-1} was determined by integration (and normalized to out of plane bending vibration of para substituted benzene ring at 830 cm^{-1}). This approach follows evaluation suggested in literature to determine general cure rate of epoxy thermosets[42,43]; numerical data from this procedure are summarized in Table I. Integration of the oxirane band at 915 cm^{-1} for ATR-FTIR traces IB through IIIB of Figure 4(b) followed the sequence IIB > IB ~ IIIB. This sequence indicated that the highest remaining oxirane group concentration was observed for the composite with 1 wt % poly(HEMA)/MWCNT concentration while lowest for 0.15 wt % content which was equivalent for neat epoxy.

ATR-FTIR experiments indicated that crosslink formation and crosslink structures are different for epoxy composite setups when oxirane group conversion is used as qualitative measure.

Table I. Integrated Bands for Evaluation of Conversion Reaction/Crosslink Formation for Epoxy Composites

Epoxy composite type	Integrated OH band at 3380 cm^{-1} (au)	Integrated oxirane group band at 915 cm^{-1} (au)
0.15 wt % poly(HEMA)/MWCNT	0.10	0.02
1 wt % poly(HEMA)/MWCNT	0.42	0.05
Neat epoxy	1.21	0.02

Applied Polymer SCIENCE

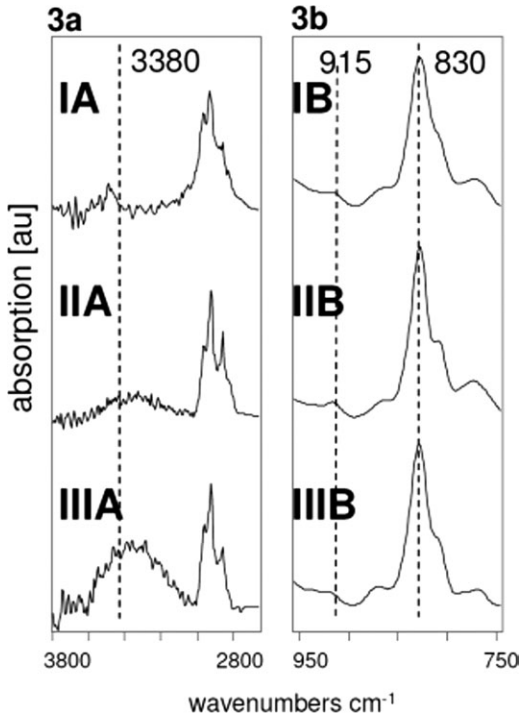

Figure 6. ATR-FTIR spectra of poly(HEMA)/MWCNT containing epoxy composites with 0.15 wt % (I) and with 1 wt % (II) compared with neat epoxy (III). Traces "A" illustrate OH functional group and "B" oxirane functional group content in epoxy/composites.

Because 1 wt % poly(HEMA) MWCNT composites indicated the lowest conversion (and highest remaining oxirane content), curing appears to be reduced for elevated concentration of modified MWCNT; therefore, reduced concentrations of this additive type employed in potential technical composites appear to be favorable.

Mechanical Analysis

The cast poly(HEMA)-MWCNT/epoxy plaques containing 0, 0.15, and 1.0 wt % poly(HEMA)-coated MWCNTs were evaluated for mechanical strength. The force-deformation curves were obtained from 5 specimens per loading of poly(HEMA)-MWCNT (0, 0.15, and 1.0 wt %) and characterized for properties relating to the proportional limit, yield point, and toughness (Table II).

Mechanical analysis indicated that the poly(HEMA)-MWCNT/epoxy composite containing 0.15 wt % possessed the highest mechanical properties for stress and strain at the proportional limit (PL) and maximum stress and strain for the systems evaluated in this study (Table II). However, the Young's Modulus of the composite of both the poly(HEMA)-MWCNT and the neat system were within ~2%. Although a major objective of carbon nanotube studies is to enhance the Young's Modulus of a system, increasing the ultimate tensile strength of a composite while retaining similar stiffness properties enables CNT-modified systems to be utilized in the same applications as intended with higher performance. Mechanical analysis indicated that the epoxy composites did not undergo plastic deformation under the conditions employed indicating that the increase in toughness observed was induced by a different mechanism. The increase in toughness can then be attributed to an increase in load transfer from the matrix to the MWCNT. These results indicate that more research should be performed for MWCNT concentrations near 0.15 wt % for determination of the optimal carbon nanotube loading.

Hardness

The hardness of each system was measured with a Shore D durometer to observe the effect incorporating functionalized MWCNTs (Table III). Each measurement was obtained from a specimen of the plaques used for mechanical analysis to ensure that the substrate did not influence the results. The hardness of each system behaved similarly to the mechanical properties observed above; the 0.15 wt % functionalized MWCNT had the highest hardness and the neat and 1.0 wt % composite types had similar values (Table III).

Thermal Gravimetric Analysis

Characterization of the functionalized MWCNTs indicated that they are comprised of ~30 wt % poly(HEMA).

The addition of poly(HEMA)-MWCNTs at 0.15 wt % will increase thermal stability of the system as observed in Figure 7 using thermogravimetric analysis. At a 1.0 wt % loading of the poly(HEMA)-MWCNTs, thermal stability of the system decreased compared to the neat epoxy system (Table IV); this

Table II. Mechanical Properties of Poly(hydroxyethyl methacrylate)-Coated Multiwalled Carbon Nanotube-Epoxy Composites

Stress strain @ PL (MPa)	Max @ PL (mm/mm)	Max Stress (MPa)	Young's Strain (mm/mm)	Modulus (MPa)	Toughness (MJ/m^3)	
Neat						
Ave	54.8	0.053	54.8	0.053	1036.9	1.8
Stdev	4.4	0.005	4.4	0.005	44.7	0.3
0.15 wt %						
Ave	62.3	0.061	63.2	0.062	1028.4	2.3
Stdev	4.8	0.005	4.7	0.005	45.3	0.4
1.0 wt %						
Ave	56.1	0.054	56.1	0.054	1033.8	1.6
Stdev	1.6	0.001	1.6	0.001	29.1	0.3

Table III. Shore D Hardness of Poly(hydroxyethyl methacrylate)-Coated Multiwalled Carbon Nanotube-Epoxy Composites

Epoxy composite type	Shore D hardness	Std deviation
Neat	82	5
0.15	87	5
1%	83	15

behavior was also observed when investigating the mechanical properties (Table II) and can be attributed to stoichiometric imbalance caused by the increased concentration of hydroxyl groups from the functionalized MWCNTs or incomplete conversion of the crosslinking system due to steric hindrance of the poly(HEMA)-coated MWCNT during the cure.

Differential Scanning Calorimetry

The DSC scans indicated that none of the specimens analyzed were fully cured despite utilizing the manufacturers' cure schedule. As a result, an increase in the glass transition was observed upon the second heating scan when compared with the peak signal of the physical aging peak due to increased cure. However, the main objective of this research was to incorporate commercially viable functionalized MWCNTs into a commercially available system according to the recommended cure schedule; thus, the systems studied here should accurately replicate the physical properties when employed in real world applications. The maximum signal, glass transition temperature from the cooling cycle, and glass transition from the heating cycle are found in Table V.

The glass transition temperature of a thermosetting polymer is directly dependent on the crosslink density, number of free chain ends, and rigidity of polymeric segments, and has been the subject of previous research.[44,45] The poly(HEMA)-MWCNTs introduced to the epoxy system leads to an increase in chain ends and free volume in the system, from poly(-HEMA), unreacted TETA and the epoxy resin, which should alter the glass transition temperature. However, differential scanning calorimetry indicated no observable change in the glass transition temperature of the resin system utilized in this study when incorporating poly(HEMA)-MWCNTs at a concentration of 0.15 wt %. The composite that contained 1.0 wt % poly (HEMA)-MWCNTs was observed to have a lower T_g and physical aging peak when compared to neat resin; this may be attributed to an increased amount of free chain ends and stoichiometry imbalance of the additional functional groups of the poly(HEMA)-MWCNTs.

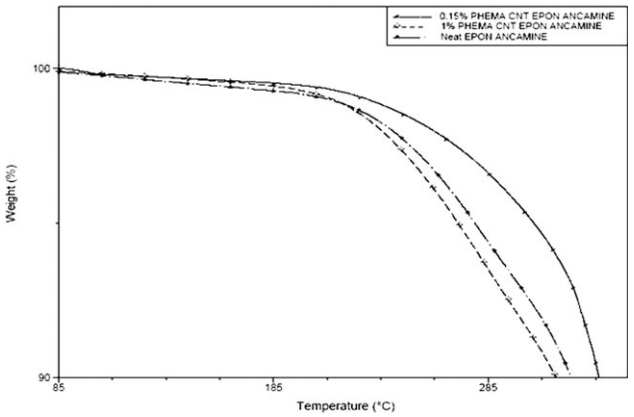

Figure 7. Representative thermograms of EPON 8111/TETA epoxy samples that were functionalized by poly(HEMA)-multiwalled carbon nanotubes at 0, 0.15, and 1.0 wt %.

Scanning Electron Microscopy

The surface roughness of a fracture material can bring insight into the mechanism of crack propagation through the material. In general, the rougher the surface, the more tortuous path the crack must propagate during the fracture event.[16–18,26,39] When a crack initiates, propagation occurs along the plane of least resistance (typically matrix defects) until a portion of the matrix has sufficient energy to stop or deflect propagation.

The moieties that alter crack propagation in the system used in this study can be either chemical bonds or functionalized MWCNT (if present in the matrix). To observe crack propagation during the fracture event, the fractured surfaces were investigated using SEM at 500 and 2000x magnification (Figure 8).

The surface morphology of the neat epoxy after fracture had several smooth structures when observed at 2000x [Figure 8(b)]. These structures appear throughout the fractured surface

Table IV. Thermogravimetric Measurements of poly(HEMA)-MWCNT/epoxy Nanocomposites at Various Heating Rates

Sample	2% Weight Loss	5% Weight Loss	10% Weight Loss	Derivative Onset 1	Derivative Onset 2	Derivative Peak
20°C/min						
Neat						
Average	238	278	318	200	325	369
St Dev	11	14	10	5	7	3
0.15 wt %						
Average	245	287	326	206	327	372
St Dev	10	15	9	5	3	8
1.0 wt %						
Average	232	269	312	201	328	371
St Dev	8	13	19	3	3	2

Applied Polymer SCIENCE

Table V. Thermal Transitions of Poly(hydroxyethyl methacrylate)-Functionalized Multiwalled Carbon Nanotube-Epoxy Composites

Sample	Endotherm Peak	T_g cool	T_g
Neat			
Average	58.53	57.87	62.36
Std Dev	0.22	0.79	1.13
0.15 wt %			
Average	58.49	57.68	62.16
Std dev	0.60	1.45	1.32
1.0 wt %			
Average	55.79	53.73	58.48
Std dev	0.49	0.57	0.85

as shown by the images obtained at 500x [Figure 8(a)]; the presence of these structures indicates that there were several planes where the crack was relatively free to propagate. The poly(HEMA)-MWCNT/epoxy composite at 0.15 wt % loading qualitatively contained much smaller and more numerous smooth sections on the fractured surface when compared to the neat epoxy. This can be attributed to crack propagation being either stopped or deflected due to the presence of well dispersed MWCNTs with enhanced interaction with the epoxy matrix. This behavior of crack propagation in the 0.15 wt % poly (HEMA)-MWCNT/epoxy system follows the mechanical properties as described above. The surface morphology of the 1.0 wt % poly(HEMA)-MWCNT/epoxy composite is very different from those observed in the neat and 0.15 wt % poly(HEMA)-MWCNT/epoxy systems. This can be attributed to agglomeration of the MWCNTs due to higher MWCNT concentration within the matrix or an increase of free volume due to more chain ends within the polymer matrix.

CONCLUSIONS

Purified multiwalled carbon nanotubes were chemically functionalized by a surface initiated polymerization of 2-hydroxyethyl methacrylate using BPO. The poly(HEMA)-MWCNTs were incorporated into a commercially available epoxy resin and the thermal and mechanical properties were investigated. Strips of poly(HEMA)-MWCNTs/epoxy were cut via waterjet from cast plaques. Mechanical analysis indicated an ultimate tensile strength approximately 30% higher at a poly(HEMA)-MWCNT loading of 0.15 wt % when compared with the neat resin, yet a similar Young's modulus. The fractured surfaces of the tensile experiments were examined by scanning electron microscopy; the surface of the 0.15 wt % was found to possess a rougher surface when compared to the neat and 1.0 wt % specimens. These results indicate that the poly(HEMA)-coated MWCNTs have good interfacial interaction with the epoxy resin. The glass transition temperature of the 0.15 wt % was found to be nearly the same as the neat epoxy polymer whereas the T_g of the 1.0 wt % was slightly lower compared to the neat epoxy. The effects of varying functionalization parameters (i.e. initiator concentration, sonication time, polymerization time, monomer composition) and carbon nanotube concentrations must be better understood to synthesize functionalized MWCNTs for optimal properties for various applications.

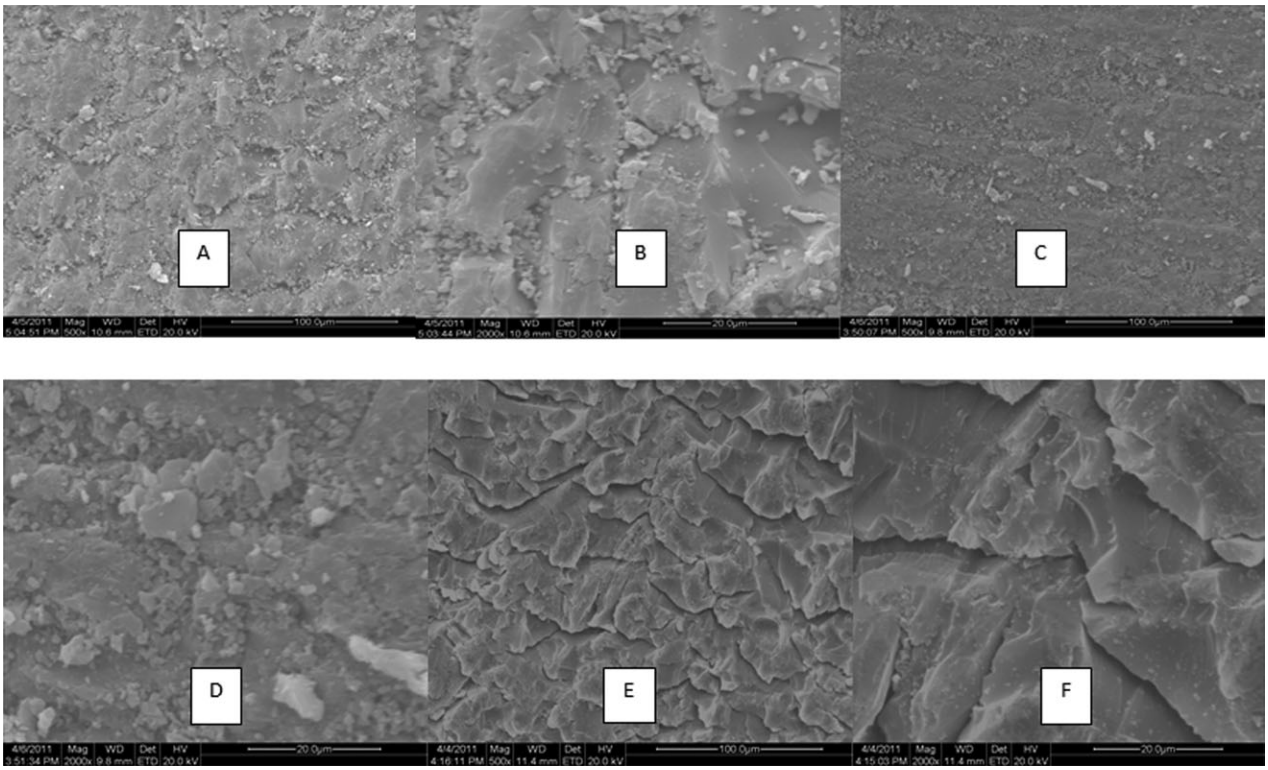

Figure 8. SEM image of neat epoxy at 500× (a) and 2000× (b), 0.15 wt % at 500× (c), and 2000× (d), and 1.0 wt % at 500× (e) and 2000× (f).

ACKNOWLEDGMENTS

The authors would like to thank the California Central Coast Research Partnership (C3RP) for providing funding to complete the project, California Polytechnic State University, San Luis Obispo, and the University of Southern Mississippi and Dr. William Jarrett for instrumentation advice.

REFERENCES

1. Coleman, J. N.; Khan, U.; Blau, W. J.; Gun'ko, Y. K. *Carbon* **2006**, *44*, 1624.
2. Ugur, S.; Yargi, O.; Pekcan, O. *Procedia Eng.* **2011**, *10*, 1709.
3. Chou, T.-W.; Gao, L.; Thostenson, E. T.; Zhang, Z.; Byun, J.-H. *Compos. Sci. Technol.* **2010**, *70*, 1.
4. Gojny, F. H.; Wichmann, M. H. G.; Köpke, U.; Fiedler, B.; Schulte, K. *Compos. Sci. Technol.* **2004**, *64*, 2363.
5. Kim, Y. S.; Kim, D.; Martin, K. J.; Yu, C.; Grunlan, J. C. *Macromol. Mater. Eng.* **2010**, *295*, 431.
6. Jurewicz, I.; Worajittiphon, P.; King, A. A. K.; Sellin, P. J.; Keddie, J. L.; Dalton, A. B. *J. Phys. Chem. B* **2011**, *115*, 6395.
7. Burghard, M. *Surface Sci. Rep.* **2005**, *58*, 1.
8. Spitalsky, Z.; Tasis, D.; Papagelis, K.; Galiotis, C. *Prog. Polym. Sci.* **2010**, *35*, 357.
9. Li, X.; Wong, S. Y.; Tjiu, W. C.; Lyons, B. P.; Oh, S. A.; He, C. B. *Carbon* **2008**, *46*, 829.
10. Xia, H.; Qiu, G.; Wang, Q. *J. Appl. Polym. Sci.,* **2006**, *100*, 3123.
11. Lu, J.; Feller, J. F.; Kumar, B.; Castro, M.; Kim, Y. S.; Park, Y. T.; Grunlan, J. C. *Sens. Actuators, B* **2011**, *B155*, 28.
12. Kyrylyuk, A. V.; Hermant, M. C.; Schilling, T.; Klumperman, B.; Koning, C. E.; van, d. S. P. *Nat. Nanotechnol.* **2011**, *6*, 364.
13. Grossiord, N.; Loos, J.; Regev, O.; Koning, C. E. *Chem. Mater.* **2006**, *18*, 1089.
14. Bose, S.; Bhattacharyya, A. R.; Khare, R. A.; Kulkarni, A. R.; Patro, T. U.; Sivaraman, P. *Nanotechnology* **2008**, *19*, 335704/1.
15. Bose, S.; Khare, R. A.; Moldenaers, P. *Polymer* **2010**, *51*, 975.
16. Ayatollahi, M. R.; Shadlou, S.; Shokrieh, M. M.; Chitsazzadeh, M. *Polym. Test.* **2011**, *30*, 548.
17. Sun, L.; Gibson, R. F.; Gordaninejad, F.; Suhr, J. *Compos. Sci. Technol.* **2009**, *69*, 2392.
18. Hernández-Pérez, A.; Avilés, F.; May-Pat, A.; Valadez-González, A.; Herrera-Franco, P. J.; Bartolo-Pérez, P. *Compos. Sci. Technol.* **2008**, *68*, 1422.
19. Ma, P.-C.; Siddiqui, N. A.; Marom, G.; Kim, J.-K. *Compos. Part A: Appl. Sci. Manufact.* **2010**, *41*, 1345.
20. Xie, X.-L.; Mai, Y.-W.; Zhou, X.-P. *Mater. Sci. Eng. R: Rep.* **2005**, *49*, 89.
21. Sahoo, N. G.; Rana, S.; Cho, J. W.; Li, L.; Chan, S. H. *Prog. Polym. Sci.* **2010**, *35*, 837.
22. Grossiord, N.; Regev, O.; Loos, J.; Meuldijk, J.; Koning, C. E. *Anal. Chem.* **2005**, *77*, 5135.
23. Grossiord, N.; van, d. S. P.; Meuldijk, J.; Koning, C. E. *Langmuir* **2007**, *23*, 3646.
24. Mirjalili, V.; Hubert, P. *Compos. Sci. Technol.* **2010**, *70*, 1537.
25. Kostopoulos, V.; Baltopoulos, A.; Karapappas, P.; Vavouliotis, A.; Paipetis, A. *Compos. Sci. Technol.* **2010**, *70*, 553.
26. Gojny, F. H.; Wichmann, M. H. G.; Fiedler, B.; Schulte, K. *Compos. Sci. Technol.* **2005**, *65*, 2300.
27. Gojny, F. H.; Nastalczyk, J.; Roslaniec, Z.; Schulte, K. *Chem. Phys. Lett.* **2003**, *370*, 820.
28. Zhang, W.; Picu, R. C.; Koratkar, N. *Nanotechnology* **2008**, *19*, 285709.
29. Granier, A.; Nguyen, T.; Steffens, K. L.; Lee, H.-J.; Shapiro, A.; Martin, J. W. International Coatings Expo: Clean-Lean-Green: Innovative Solutions for the Global Coatings Community, Toronto, ON, Canada, **2007**, pp 41/1.
30. Wu, H.-X.; Tong, R.; Qiu, X.-Q.; Yang, H.-F.; Lin, Y.-H.; Cai, R.-F.; Qian, S.-X. *Carbon* **2007**, *45*, 152.
31. Grossiord, N.; Loos, J.; Meuldijk, J.; Regev, O.; Miltner, H. E.; Van, M. B.; Koning, C. E. *Compos. Sci. Technol.* **2007**, *67*, 778.
32. Curtzwiler, G.; Costanzo, P. J.; Fernando, R.; Danes, J. E.; Vorst, K. *J. Appl. Polym. Sci.* **2011**, *121*, 964.
33. Sun, L.; Warren, G. L.; O'Reilly, J. Y.; Everett, W. N.; Lee, S. M.; Davis, D.; Lagoudas, D.; Sue, H. J. *Carbon* **2008**, *46*, 320.
34. Ganguli, S.; Aglan, H.; Dennig, P.; Irvin, G. *J. Reinf. Plast. Compos.* **2006**, *25*, 175.
35. Yaping, Z.; Aibo, Z.; Qinghua, C.; Jiaoxia, Z.; Rongchang, N. *Mater. Sci. Eng. A* **2006**, *435*, 145.
36. Qian, H.; Kalinka, G.; Chan, K. L. A.; Kazarian, S. G.; Greenhalgh, E. S.; Bismarck, A.; Shaffer, M. S. P. *Nanoscale* **2011**, *3*, 4759.
37. Haris, A.; Adachi, T.; Araki, W. *Mater. Sci. Eng. A* **2008**, *496*, 337.
38. Ayatollahi, M. R.; Shadlou, S.; Shokrieh, M. M. *Eng. Fracture Mech.* **2011**, *78*, 2620.
39. Ganguli, S.; Bhuyan, M.; Allie, L.; Aglan, H. *J. Mater. Sci.* **2005**, *40*, 3593.
40. D3418-03, A. S.; ASTM International, West Conshohocken, PA: 2003.
41. O'Brien, R. N.; Hartman, K. *J. Polym. Sci. Part C: Polym. Symp.* **1971**, *34*, 293.
42. Dannenberg, H.; Harp, W. R. *Anal. Chem.* **1956**, *28*, 86.
43. Fountain, R. *Polym. Eng. Sci.* **1974**, *14*, 597.
44. van Ekeren, P. J.; Cheng, S. Z. D., Ed.; Elsevier Science B.V., Amsterdam: 2003.
45. Hiemenz, P.; Lodge, T. In: Polymer Chemistry; Taylor and Francis Group: Boca Raton, FL, **2007**.